Received: 15 October 2021 | Revised: 28 January 2022 | Accepted: 17 February 2022

DOI: 10.1002/jbm.a.37376

RESEARCH ARTICLE

Society For Biomaterials | WILEY

Shape memory polymer hydrogels with cell-responsive degradation mechanisms for Crohn's fistula closure

Henry T. Beaman[1] | Bryanna Howes[2] | Priya Ganesh[1] | Mary Beth Browning Monroe[1]

[1]Department of Biomedical and Chemical Engineering, Syracuse BioInspired Institute, Syracuse University, Syracuse, New York, USA

[2]Department of Chemistry, LeMoyne College, Syracuse, New York, USA

Correspondence
Mary Beth Browning Monroe, Department of Biomedical and Chemical Engineering, BioInspired Syracuse: Institute for Material and Living Systems, Syracuse University, 318 Bowne Hall, Syracuse, NY 13244, USA.
Email: mbmonroe@syr.edu

Abstract

Crohn's disease, a form of inflammatory bowel disease, commonly results in fistulas, tunneling wounds between portions of the urinary, reproductive, and/or digestive systems. These tunneling wounds cause pain, infection, and abscess formation. Of Crohn's patients with fistula formation, 83% undergo surgical intervention to either drain or bypass the fistula openings, and ~23% of these patients ultimately require bowel resections. Current treatment options, such as setons, fibrin glues, and bioprosthetic plugs, are prone to infection, dislodging, and/or require a secondary removal surgery. Thus, there is a need for fistula filling material that can be easily and stably implanted and then degraded during fistula healing to eliminate the need for removal. Here, the development of a shape memory polymer hydrogel foam containing polyvinyl alcohol (PVA) and cornstarch (CS) with a disulfide polyurethane crosslinker is presented. These materials undergo controlled degradation by amylase, which is present in the digestive tract, and by reducing thiol species such as glutathione/dithiothreitol. Increasing CS content and using lower molecular weight PVA can be used to increase the degradation rate of the materials while maintaining shape memory properties that could be utilized for easy implantation. This material platform is based on low-cost and easily accessible components and provides a biomaterial scaffold with cell-responsive degradation mechanisms for future potential use in Crohn's fistula treatment.

KEYWORDS
Crohn's disease, hydrogels, shape memory polymer, starch

1 | INTRODUCTION

Fistulas are abnormal connections between the digestive, urinary, and/or reproductive system that form due to intestinal bowel disease (IBD), childbirth, surgical complications, or cancer.[1] Crohn's disease is the most common type of IBD, affecting >1,000,000 people in the United States and Europe alone, primarily between the ages of 15 and 30[2]; almost 20% of Crohn's disease patients already have a fistula at the time of their diagnosis, and ~35% of Crohn's patients develop fistulas at some point.[3] These tunneling sores cause pain, infection, and abscess formation and can ultimately lead to fecal incontinence, anal stenosis, or sepsis.[4]

Current treatment options for intestinal fistulas include antibiotics; setons; bowel restrictive surgery; and fistula fillers, such as fibrin-based glues.[5–7] Over 80% of Crohn's fistula patients undergo surgery to drain or bypass the fistula openings.[8] Surgery has short-term effectiveness, but ~23% of these patients ultimately require bowel resections, in which a portion of the colon or rectum is surgically removed.[8] Setons are effective treatment options for anal fistula closure, but involve a second removal procedure and negatively affect fecal continence.[9] An alternate treatment approach is to fill fistulas to seal off the openings and allow healing. Fibrin-based glues are an improvement to bowel restrictive surgery, as they are minimally invasive and easily applied; yet, they are prone to infection and dislodgement.[6,10]

More recently, the development of bioprosthetic plugs has been explored as a potential treatment. These materials are often comprised of lyophilized porcine submucosa, which has inherent biocompatibility, biodegradability, and host cell repopulation.[11] Bioprosthetic plugs still have failure rates of ~44%, in part due to infectious abscess formation.[12] Other plugs have been developed using synthetic polymers, such as Gore Bio-A® Fistula Plug, which is made of poly (trimethylene carbonate). This material has demonstrated biocompatibility and biodegradability[13]; however, material degradation is slow, ranging up to 6 months, and is non-specific via hydrolytic and enzymatic degradation.[14] This degradation time frame is much longer than reported fistula healing times of 2–8 weeks, and the Gore product has been discontinued.[12] Thus, there remains a clinical need for new biomaterials that can be implanted using minimally invasive procedures to stably fill the fistula site and that degrade within clinically-relevant time frames in response to healing.

Shape memory polymer (SMP) hydrogels are good candidates for the development of new fistula plugs. SMPs are materials that can be synthesized in a primary shape and, upon contact with an external stimulus, can be deformed and stored in a secondary shape after removal of that stimulus. When a second stimulus is applied, the polymer will return to its original shape. Often the stimulus used for this class of materials is heat, but other stimuli can be used, such as pH, light, magnetic field, and water. SMPs have been previously developed for use in a range of biomedical applications, such as dermal wounds, aneurysms, and traumatic wounds.[15–18] For fistula filling, porous SMP foam cylinders could be applied non-invasively in a compressed, low-profile shape. Then, once the stimulus is applied after implantation, the cylinders could expand to fill the fistula, Figure 1. An ideal fistula treatment would then degrade in response to healing to avoid a second removal procedure. The fistula environment is moist; thus, a biodegradable hydrogel material that is highly hydrated would likely be beneficial for healing.

Biodegradable hydrogels have been previously synthesized with synthetic and natural polymers and are often based on enzymatically-degradable peptide incorporation, naturally biodegradable polymers, hydrolytically-labile bonds, or disulfide bonds.[19–21] For example, common synthetic hydrogel materials, such as polyethylene glycol (PEG) and polyvinyl alcohol (PVA), can be modified with hydrolytic, enzymatic, or thiol reductive components to enable biodegradation.[22,23] Hydrolytic degradation is often slower than the wound healing rate and it is non-specific. Enzymatic degradation via peptide incorporation relies upon expensive and time-consuming solid-phase peptide synthesis, which can hinder peptide sequence length increases to improve specificity.[20] Natural polymers, such as polysaccharides (e.g., chitosan, starch, and hyaluronic acid) are also commonly employed as enzymatically degradable elements.[24–26] Polysaccharide hydrogels generally have poor mechanical properties, but they can be combined with synthetic polymers, such as PVA, to improve scaffold tunability.[27]

Previously, PVA/starch hydrogels were formed using freeze–thaw methods or glutaraldehyde crosslinking, which provided materials with limited stability and swelling.[28–31] Here, we present a method of fabricating salt-leached PVA/starch polyurethane foams that are crosslinked using a diisocyanate-terminated disulfide crosslinker (DSX). PVA is hydrophilic and commonly employed in biomedical applications; however, crosslinked PVA is biostable. Cornstarch (CS) can degrade by amylase present in the intestines where Crohn's fistulas form; thus, the combination of PVA and CS enables healing-responsive scaffold breakdown after implantation.[32] Both PVA and CS are low-cost materials that are easy to access, and they have high synthetic tunability, making them good candidates for chemical modification. Using commercially available diisocyanates, often used in polyurethane synthesis, PVA and CS can be crosslinked into a stable 3D network using their free hydroxyl groups. To further accelerate cell-responsive degradation, disulfides can be incorporated into the diisocyanate linkers. These groups degrade in the presence of reducing thiol species, such as dithiothreitol (DTT) and biologically-available glutathione, providing an additional level of control over biodegradation rates.

The combination of CS with PVA within a polyurethane network allows tuning of scaffold properties to match those of native tissue,

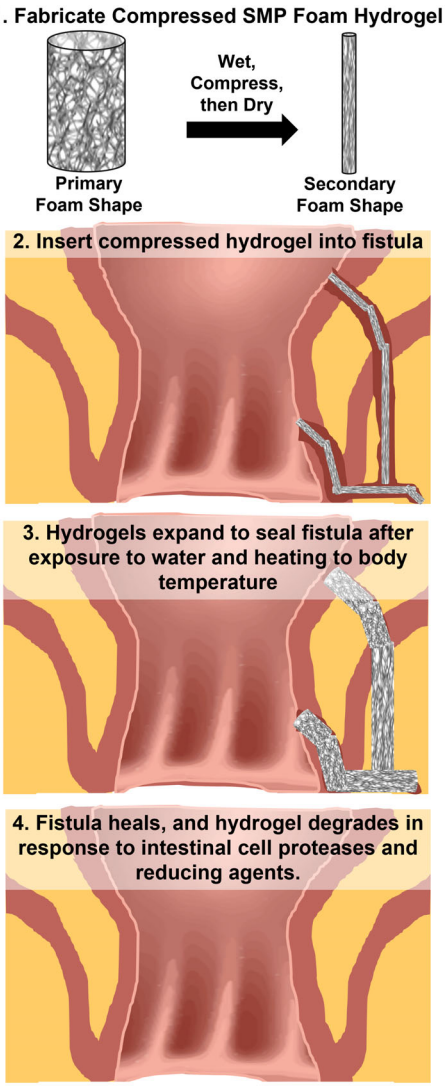

FIGURE 1 Schematic representation of proposed degradable shape memory polymer hydrogel foam fistula closure device

and the resulting shape memory polyurethane networks have high shape stability and recovery ratios. By fabricating porous foams from these materials, easy implantation of compressed, low-profile scaffolds that expand to fill defect sites after placement and that serve as a substrate for cellular infiltration during healing could be achieved. The use of these combined material components could facilitate development of an easy-to-implant, completely biodegradable system with advantages over current clinical options for fistula repair. Namely, the shape memory properties could improve material implantation and stability within the fistula in comparison with fibrin glue and bioprosthetic plugs, the degradability removes the need for explantation in comparison with setons, and the overall synthetic tunability of the system enables easy control over scaffold properties and/or introduction of new functionalities in future work, such as cell or drug delivery mechanisms and antimicrobial properties. This work examines the initial development of this material system, in which the effects of hydrogel chemistry (varying ratios of CS:PVA and PVA molecular weight) on degradation, thermal and mechanical properties, shape memory, and cytocompatibility are characterized to enable future development of clinically-relevant fistula filling scaffolds.

2 | METHODS

2.1 | Materials

CS, hexamethylene diisocyanate (HDI), dimethyl sulfoxide, sodium chloride (NaCl), and DTT were all purchased from Fisher Scientific. 2-Hydroxyethyl disulfide (HEDS) was purchased from TCI Chemicals (Portland, OR). PVA of two different molecular weight (25,000 and 6000 Da) was purchased from Polysciences (Warrington, PA). All cell culture solutions and chemical were purchased from ThermoFisher (Waltham, MA).

2.2 | Synthesis

2.2.1 | Disulfide crosslinker

A polyurethane DSX was synthesized using HEDS and HDI, Figure 2. Monomers were placed into a round bottom flask in a humidity-controlled glove box at a molar ratio of 2:1 (HDI:HEDS). DMSO dried over molecular sieves was added to the round bottom flask in a mass (g) to volume (ml) ratio of 0.73:1 (monomers:DMSO). The reaction was maintained at 50°C with constant stirring under nitrogen until Fourier transform infrared (FTIR) spectroscopy confirmed a complete reduction of hydroxyl peak (~3200–3500 cm^{-1}). DSX was then stored within the glove box for further use.

2.2.2 | Hydrogel films

Previously weighed CS and PVA were dissolved in DMSO (dried over molecular sieves) at 90°C under nitrogen to make a 10% solution (w/v). Once completely dissolved, the solutions were allowed to cool to room temperature. DSX was added to a speed mixing cup inside the glove box. The PVA/CS mixtures were then combined in varying ratios with the DSX outside of the glove box. The DSX:polyol weight ratio was 0.364:1. The hydrogel components

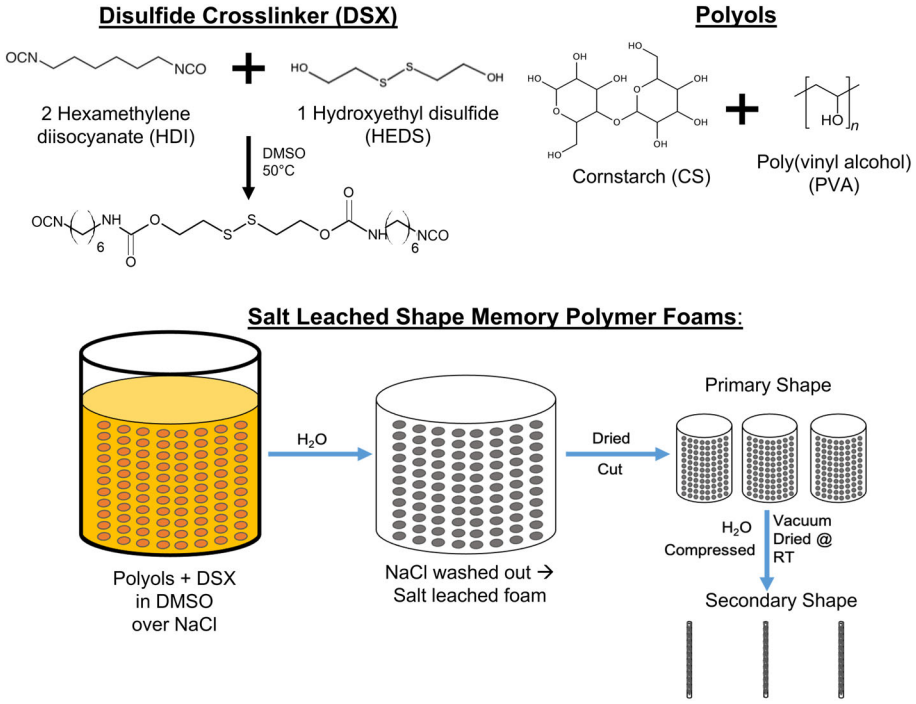

FIGURE 2 Schematic overview of starch/PVA hydrogel foam synthesis. PVA, poly(vinyl alcohol)

were mixed using a Flacktek high speed mixer (Landrum, SC) at 3500 rpm for 10 s. The contents were poured into a glass petri dish and crosslinked at 50°C for 8 h. Upon completion of crosslinking, films were washed twice in deionized (DI) water for 20 min to remove any unreacted material and residual DMSO. Synthesized hydrogel formulations are shown in Table 1. Samples were air dried overnight and then further dried in a 50°C vacuum oven for 24 h. Samples were examined by FTIR after drying.

2.2.3 | Hydrogel foams

Foams were synthesized using the same protocol as the hydrogel films with the addition of vacuum dried NaCl porogens (sieved to 300–500 μm; weight ratio of 32 NaCl:1 hydrogel components) to the speed mixer cup in the mixing step, Figure 2. After mixing, samples were vortexed for 30 s, and foams were polymerized in the speed mixer cup. Foams were placed into DI water for 24 h on a 37°C shaker table at 100 rpm to remove NaCl porogens, and then vacuum dried for 24 h at 50°C. Samples were examined by FTIR after drying.

2.3 | Characterization

2.3.1 | Gel fraction

Prior to washing films with DI water, 8 mm biopsy punches were taken ($n = 3$). Samples were dried in a 50°C vacuum oven for 24 h. Samples were then weighed (W_i) and placed into a vial containing DI water. The vials were incubated at 50°C for 24 h. DI water was removed, and film pieces were vacuum dried at 50°C for 24 h. The samples were then reweighed (W_f). Gel fraction was calculated by:

$$\text{Gel fraction}\,(\%) = \frac{W_f}{W_i} \times 100\%.$$

TABLE 1 Synthesized hydrogel formulations with varying polyvinyl alcohol (PVA):cornstarch (CS) ratios and PVA molecular weights

Sample	PVA MW (kDa)	PVA ratio (%)	CS ratio (%)
0:1	6	100	0
	25	100	0
1:2	6	67	33
	25	67	33
1:1	6	50	50
	25	50	50
2:1	6	33	67
	25	33	67

2.3.2 | Porosity

Density of films (D_f) and foams (D_p) were measured on 6 mm biopsy punches using mass and volume measurements ($n = 3$). Porosity was determined as:

$$\text{Porosity}\,(\%) = \frac{D_p - D_f}{D_P} \times 100\%.$$

2.3.3 | Swelling

Thin hydrogel discs were collected from casted films using a 6 mm biopsy punch. Film samples ($n = 3$) were weighed in the initial dry state (W_i) then placed into vials containing 37°C DI water. Vials were incubated in a water bath at 37°C to maintain the temperature. Samples were removed from the vials and weighed (W_t) at 1, 5, 10, 30, and 60 min and at 24 h. Swelling ratio was calculated using:

$$\text{Swelling ratio} = \frac{W_t - W_i}{W_i}.$$

2.3.4 | Pore size and morphology

Foam slices ($n = 3$) for each formulation were cut and sputter coated with gold for 45 s. Foams were imaged using Jeol NeoScope JCM-5000 Scanning Electron Microscope (SEM). Pore size was determined by analyzing 50 total pores per formulation using the measuring tool in ImageJ. Pores size was reported as the average diameter of measured pores.

2.3.5 | Cytocompatibility

Caco-2 cells were cultured in Dulbecco's modified Eagle's medium supplemented with 10% fetal bovine serum and 1% Penicillin/Streptomycin (Pen/Strep). Cells were seeded into 24 well plates at a density of 5000 cells per well 1 day prior to testing. Samples ($n = 3$) weighing 10 mg (dry) were sterilized by incubating in 70% ethanol overnight and then moving into sterile phosphate buffered saline (PBS) for 3 h before placing directly into wells. Cytocompatibility was measured at 24, 72, and 168 h using a resazurin assay, in which a 10% resazurin solution (prepared in cell culture media) was added to cells and incubated for 1 h. Using a plate reader, fluorescence absorbances (excitation 530 nm and 590 emission) were obtained and compared to an untreated control. Cytocompatibility was calculated by:

$$\text{Cell viability}\,(\%) = \frac{\text{Abs}_{\text{Sample}} - \text{Abs}_{\text{Blank}}}{\text{Abs}_{\text{Control}} - \text{Abs}_{\text{Blank}}} \times 100\%.$$

2.3.6 | Mechanical properties

Film ($n = 3$) and foam ($n = 3$) samples were characterized in terms of tensile and compressive properties, respectively (Model 100P Universal Testing Machine, Test Resources, Shakopee, MN). Films were

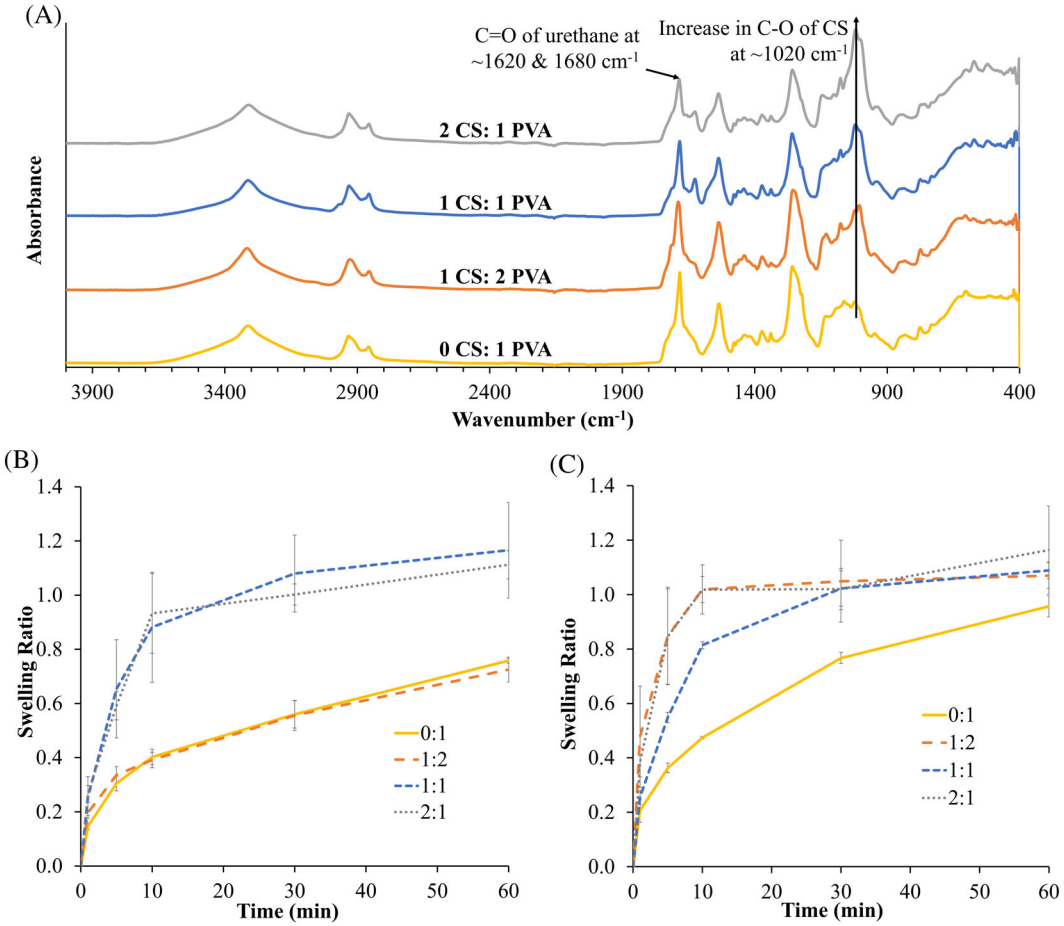

FIGURE 3 (A) Fourier transform infrared spectra of poly(vinyl alcohol) (PVA) 6k hydrogels with varied cornstarch content. Swelling profiles of (B) PVA 6k and (C) PVA 25k hydrogel films in water at 37°C. Mean ± standard deviation displayed ($n = 3$)

TABLE 2 Characterization summary of synthesized hydrogels

Formulation	0 CS:1 PVA		1 CS:2 PVA		1 CS:1 PVA		2 CS:1 PVA	
PVA Mw	6k	25k	6k	25k	6k	25k	6k	25k
Gel fraction (%)	87 ± 1	77 ± 1	84 ± 1	80 ± 3	78 ± 1	71 ± 2	86 ± 2	73 ± 2
24 h swelling ratio	1.06 ± 0.01	1.04 ± 0.02	1.07 ± 0.04	1.03 ± 0.11	1.19 ± 0.12	1.17 ± 0.06	1.18 ± 0.06	1.18 ± 0.10
Pore size (μm)	200 ± 40	220 ± 40	180 ± 40	210 ± 40	240 ± 60	200 ± 60	190 ± 50	210 ± 30
Porosity (%)	57 ± 9	71 ± 1	63 ± 5	73 ± 4	67 ± 2	73 ± 6	57 ± 7	71 ± 2

Note: Mean ± standard deviation displayed ($n = 3$).
Abbreviations: CS, cornstarch; PVA, poly(vinyl alcohol).

swollen in 37°C PBS and cut into dog bones with gauge length of 6.25 mm and width of 1.5 mm, which were stretched at a rate 5 mm/min until failure. Cylindrical foam specimens (7 mm diameter and 3.5 mm height) were compressed in the dry and wet states at 1 mm/min. Wet samples were tested directly after removal from PBS.

2.3.7 | Thermal analysis

Differential scanning calorimetry (DSC) was used to examine thermal properties. Foam samples ($n = 3$) weighing 3–5 mg were placed into aluminum T-Zero pans. Samples were subjected to the following thermal cycle: equilibration at 0°C for 2 min, heated to 180°C at 10°C/min, held isothermally for 2 min, cooled to 0°C at 10°C/min, held isothermally for 2 min, and heated to 180°C at 10°C/min. Thermal transitions were taken from the second heating cycle.

2.3.8 | Shape memory properties

Foams were placed in water for 1 h and then cut into cylindrical samples (6 mm diameter, 4 mm height, $n = 3$). After cutting, samples were

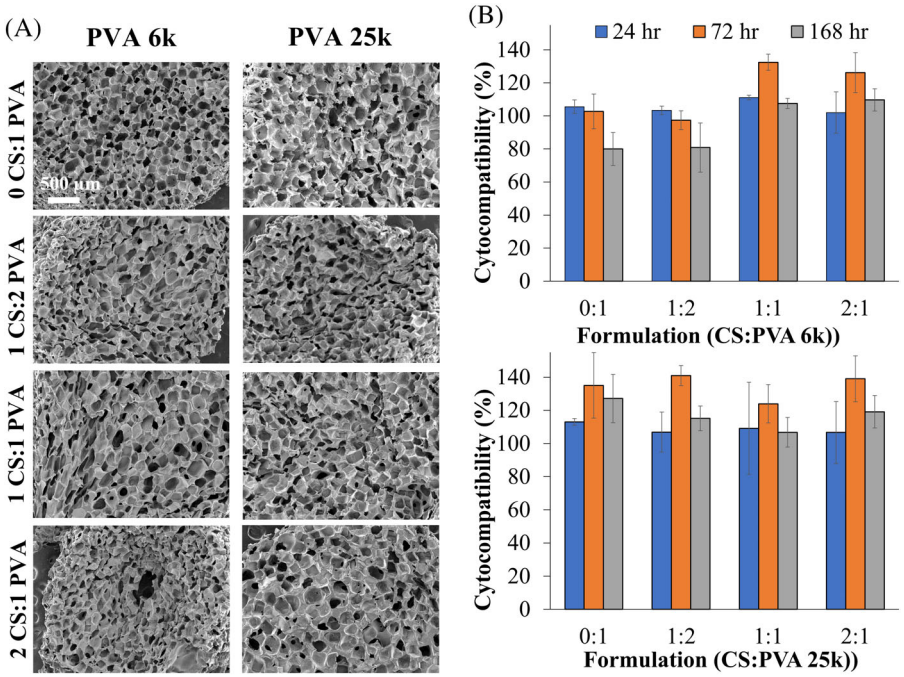

FIGURE 4 (A) Scanning electron micrographs of hydrogel foams. Scale bar applies to all images. (B) Caco-2 cytocompatibility after 24, 72, and 168 h of exposure to hydrogel films. Mean ± standard deviation displayed ($n = 3$)

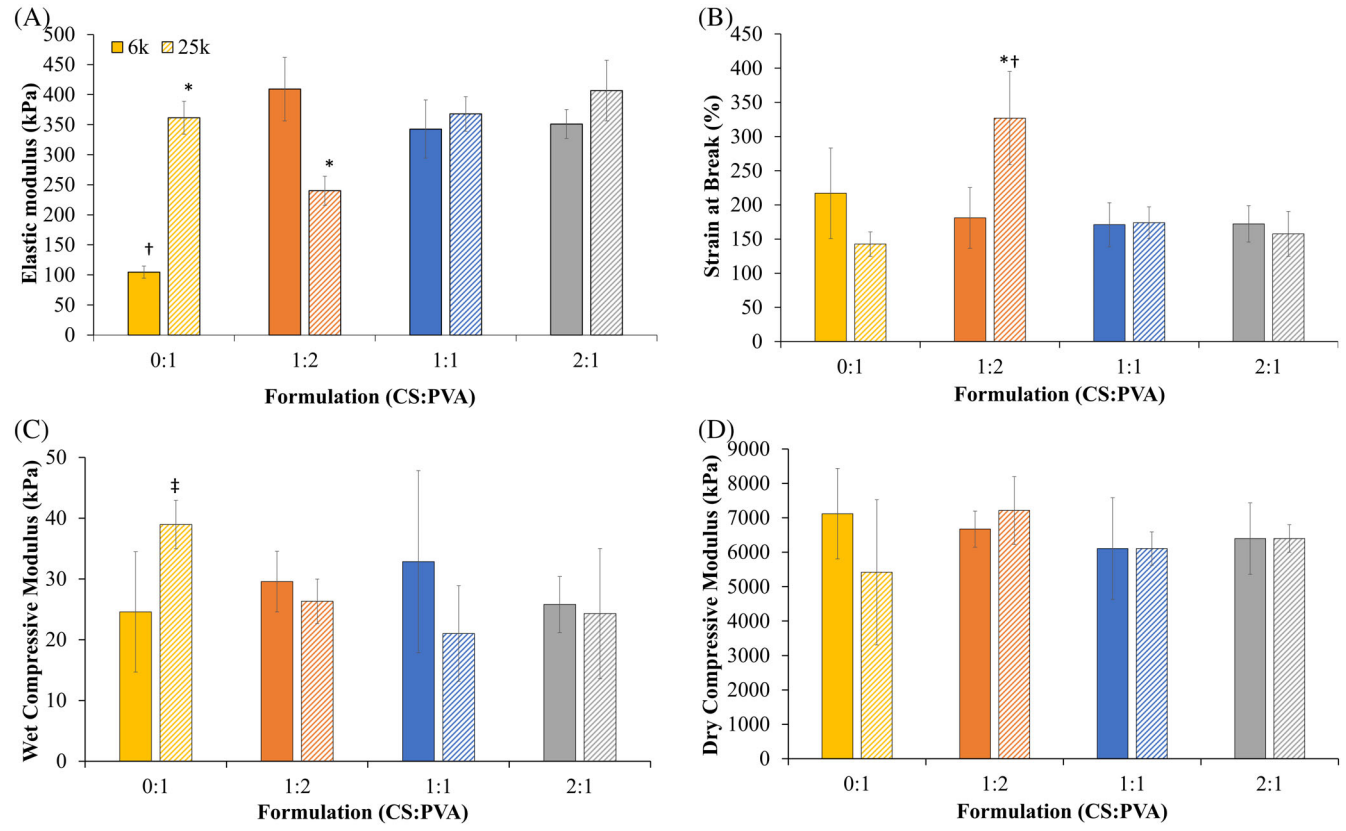

FIGURE 5 Mechanical properties of hydrogel foams and films. Film (A) elastic modulus and (B) strain at break in the wet state. Compressive modulus of foams in the (C) wet and (D) dry state. Solid bars are PVA 6k formulations and hatched bars are PVA 25k formulations. Mean ± standard deviation displayed. *$p < .05$ relative to corollary PVA 6k formulation. †$p < .05$ relative to all other formulations in the same PVA molecular weight. ‡$p < .05$ relative to 1:2 and 1:1 formulations with same PVA molecular weight ($n = 3$ for all). PVA, poly(vinyl alcohol)

radially compressed using a BlockWise radial crimper (Tempe, AZ). The crimper was then placed into a room temperature vacuum oven for 24 h to dry the samples in the compressed state. Upon removal, radius was measured (R_i) and samples were incubated at room temperature and ambient humidity for 24 h, after which samples radius was measured again (R_f). Shape fixity was calculated by:

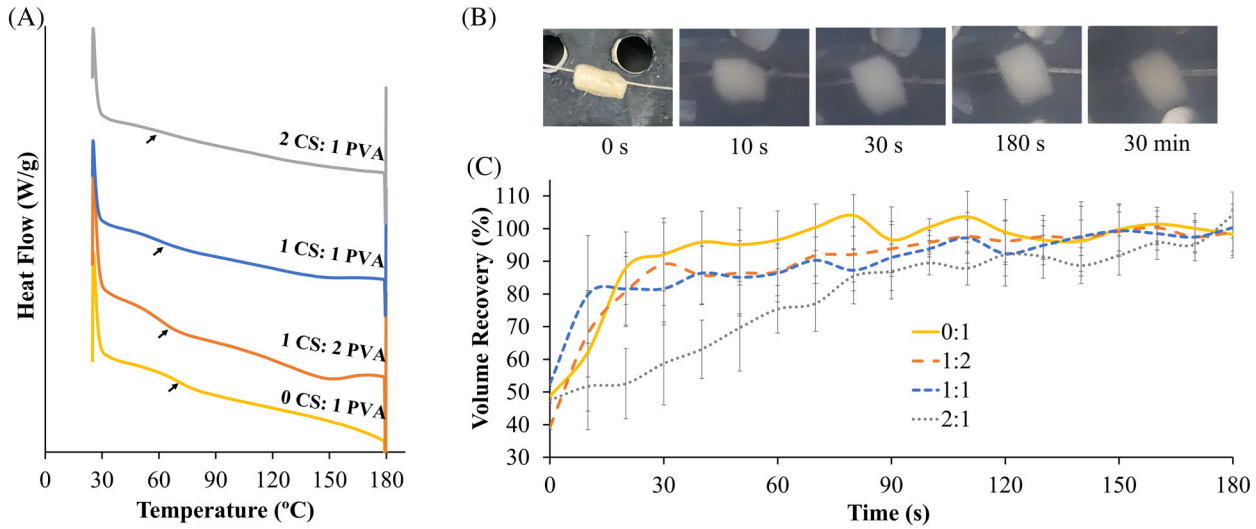

FIGURE 6 Thermal and shape memory properties of hydrogel foams. (A) Differential scanning calorimetry traces of PVA 6k foams. Arrows denote endotherms associated with glass transition (~60–85°C) temperatures (T_g). (B) Representative images of volume recovery of 0 CS:1 PVA 6k foam. (C) Volume recovery profiles of PVA 25k formulations ($n = 3$). CS, cornstarch; PVA, poly(vinyl alcohol)

$$\text{Shape fixity} = \frac{R_i - (R_f - R_i)}{R_i} \times 100.$$

Samples were then submerged in 37°C water, and images were taken every 10 s for 30 min. At 30 min, samples were removed, and diameter was measured. Using ImageJ, sample diameter (R_t) was quantified at each time point by calibrating to the 60-min water exposure length and the initial diameter (R_f). Shape recovery was calculated as:

$$\text{Shape recovery} = \frac{R_t}{R_f} \times 100.$$

2.4 | Degradation

Dry samples of each formulation ($n = 3$) weighing between 20 and 30 mg were swollen in PBS for 24 h prior to starting degradation. Samples were weighed and placed in 5 ml of PBS (control media), 10 mM DTT (disulfide degrading media), 100 U/ml amylase (CS degrading media, or 10 mM DTT + 100 U/ml amylase. All degradation solutions were prepared in PBS. Media was changed daily. Samples were weighed every 2 days for up to 20 days after lightly pressing dry for 10 s using a paper towel. Swollen mass remaining was calculated by:

$$\text{Swollen mass remaining}\,(\%) = \frac{\text{Mass}_{\text{n day}}}{\text{Mass}_{\text{Inital}}} \times 100\%.$$

2.5 | Statistical analysis

Measurements are presented as mean ± standard deviation. Student's *t*-tests were performed to determine differences between formulations, where a *p*-value of <.05 was taken as statistically significant.

3 | RESULTS

3.1 | Synthesis

The FTIR spectra of CS/PVA hydrogels (Figure 3A) showed a peak at ~1680 cm^{-1} in all formulations. This peak is associated with the urethane linkage formed between HEDS and HDI in the DSX. An increased absorbance at ~1020 cm^{-1} was observed with increasing CS content. This peak is attributed to the glycosidic ester between starch molecules (C-O-C). In addition, with increasing CS content, a peak at ~1620 cm^{-1} emerges that corresponds to the urethane linkage between the DSX and CS. These spectra confirm successful synthesis of crosslinked polyurethane-based PVA/CS hydrogels. Figure 3A shows the PVA 6k formulations; similar trends were observed in the PVA 25k hydrogel FTIR spectra.

3.2 | Characterization

In general, gel fractions in the PVA 6k formulations were higher than those in the PVA 25k hydrogels and were in the range of 78%–87% (vs. 71%–80% for PVA 25k). Hydrogels with 1:1 CS:PVA ratios had the lowest gel fraction in both sets of hydrogels. Overall, these relatively high gel fractions demonstrate successful crosslinking of PVA/CS hydrogels with the DSX.

Equilibrium swelling ratios of hydrogel films at 24 h generally increased with increased CS content in both hydrogel sets, Table 2. The molecular weight of PVA did not significantly affect swelling in any of the testing groups. Within the PVA 6k formulations (Figure 3B), those with lower CS concentrations had a slower swelling rate before achieving equilibrium. For PVA 25k hydrogels (Figure 3C), the 0:1 formulation with no CS showed the slowest swelling rate.

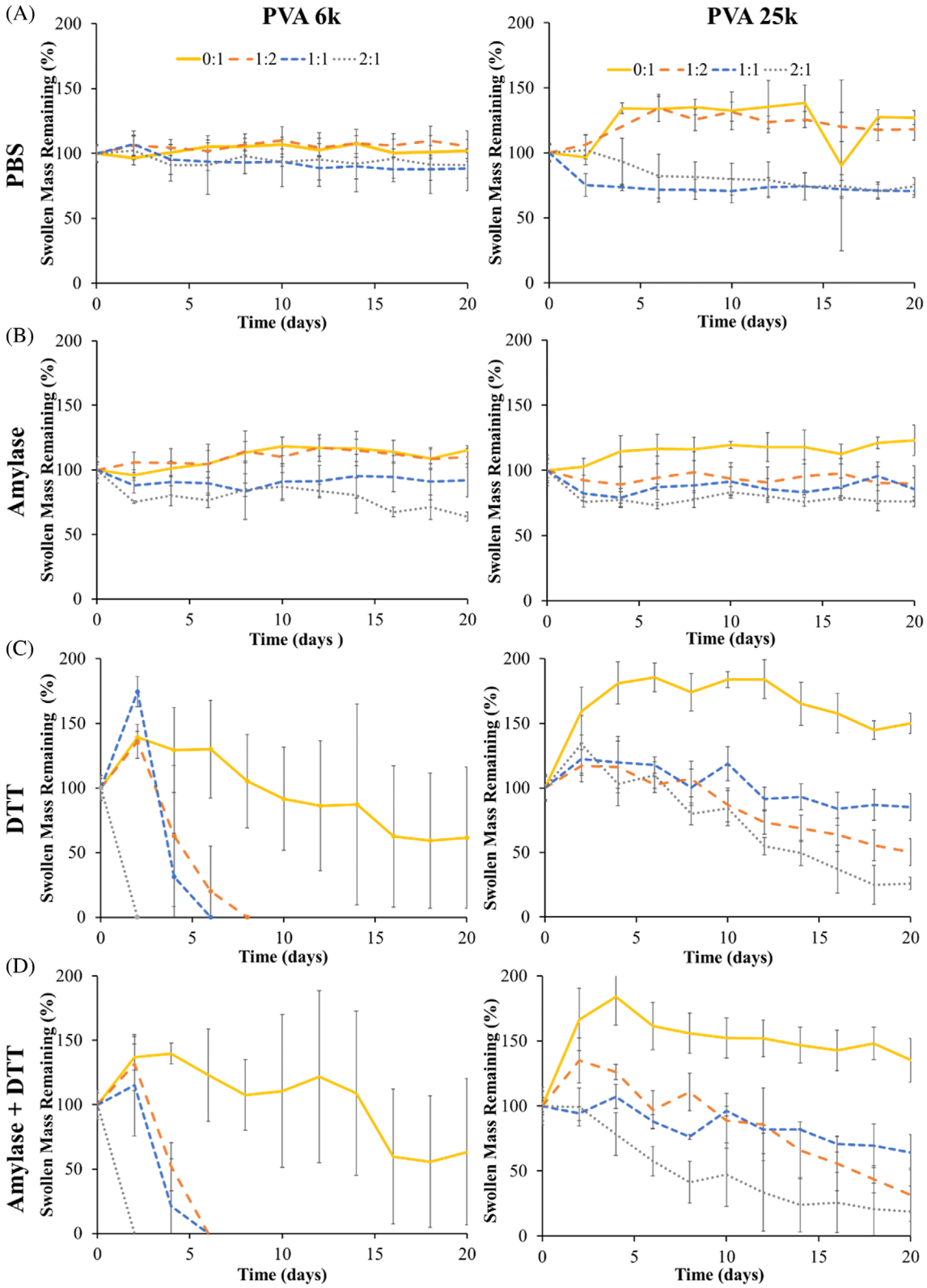

FIGURE 7 Degradation profiles (swollen mass remaining) in (A) PBS, (B) 100 U/ml amylase, (C) 10 mM DTT, and (D) 100 U/ml amylase + 10 mM DTT of (left) PVA 6k and (right) PVA 25k hydrogel foams ($n = 3$) DTT, dithiothreitol; PBS, phosphate buffered saline; PVA, poly(vinyl alcohol)

Foam pore sizes were slightly smaller on average in the majority of the PVA 6k hydrogels, but no statistically different pore sizes were measured between the formulations. Porosity was also generally lower in the PVA 6k formulations in comparison with the PVA 25k hydrogels. Within a given PVA molecular weight, no significant differences in porosity were measured, and no clear trends were observed

based on CS content. Uniform pore shape and distribution throughout the scaffolds was observed in SEM images of the foam formulations (Figure 4A).

All formulations showed Caco-2 cell cytocompatibility >80% at 24, 72, and 168 h, Figure 4B. Samples containing PVA 25k showed slightly higher cytocompatibility, with all formulations having >100% cytocompatibility in comparison with empty control wells at 24 h.

Elastic modulus measurements of 6k hydrogel films showed that with the addition of CS, the material becomes significantly stiffer (Figure 5A). The 0:1 PVA 6k hydrogels had the lowest elastic modulus of all the formulations (105 kPa, significantly lower than PVA 25k 0:1 hydrogel), with all other formulations ranging between ~340 and 400 kPa. Hydrogels synthesized with PVA 25k generally had fewer modulus variations with the addition of CS. Strain at break was similar between all formulations regardless of CS content and PVA molecular weight, with the exception of the 1:2 PVA 25k hydrogel, which had a significantly higher strain at break relative to the corollary PVA 6k hydrogel and relative to all other PVA 25k hydrogels. This result may be due to the packing structure of the polymer chains. The addition of a lower concentration of CS may have disrupted the PVA network organization, reducing overall stiffness and increasing elongation. Compressive modulus of porous hydrogel foams was generally similar between all testing groups in both the wet and dry states, Figure 5C,D. The highest wet compressive modulus was recorded in the 0:1 foams containing PVA 25k. Dry compressive moduli for all the formulations were significantly higher (>2 orders of magnitude) than in the wet state.

Hydrogel foams containing PVA 6k showed glass transition temperatures (T_g's) at ~73°C in DSC thermograms. When the molecular weight of PVA was changed to 6k, T_g dropped to ~62°C, except for the 0:1 PVA 6k foam, which had a T_g of 71°C, Figure 6A. In addition, a shallowing of the T_g step was observed with increasing starch content.

All foams had high retention of the compressed shape after 24 h, with shape fixity values between 97% and 99%. Additionally, all foam formulations showed rapid shape recovery when placed into 37°C water. Complete shape recovery to the initial wet diameter was achieved in all formulations within 180 s, Figure 6B,C. In general, shape recovery was slower with increased CS content.

3.3 | Degradation

Phosphate buffered saline was employed as a control degradation media base in these studies to enable comparison with other in vitro degradation studies in the literature and to provide an understanding of the individual effects of amylase and DTT on hydrogel degradation. No large changes in mass were seen in PVA 6k formulations in PBS over 20 days (Figure 7A, left). There were some visible changes in the mass of the PVA 25k hydrogels in PBS (Figure 7A, right). Namely, formulations containing a higher amount of PVA 25k had an increase in swelling up to ~130% after 4 days in PBS, while higher CS content foams had a decrease in swollen mass down to ~75% after 4 days.

In amylase, which can degrade CS, a general increase in mass loss was observed in higher CS content hydrogels for both PVA molecular weights, Figure 7B. When hydrogels were treated with DTT, which degrades the DSX, the PVA 6k foams underwent faster degradation than PVA 25k foams, Figure 7C. The PVA 6k foams that contained CS underwent complete degradation within 2–8 days in DTT, with the fastest degradation observed in the highest CS content foam (2:1). The 0:1 PVA 6k control had an initial increase in swollen mass followed by a steady decrease to 62% mass at 20 days. In 25k PVA formulations, the 0:1 PVA control had an increase in swelling that plateaued after 4 days. In the CS containing PVA 25k foams, there was a steady loss of mass observed for all formulations, with the slowest mass loss observed in the 1:1 formulation and faster degradation in the 1:2 and 2:1

In both PVA 6k and 25k foams, combined treatment with DTT and amylase resulted in similar mass loss trends as seen with DTT alone with faster overall mass losses in the CS-containing foams, Figure 7D. The 0:1 PVA control mass loss profiles were comparable to those obtained in DTT alone. All CS-containing PVA 6k foams had complete mass loss within 6 days, with the fastest degradation again observed in the 2:1 PVA 6k foam at 2 days. All CS-containing PVA 25k formulations underwent higher amounts of mass loss in the combined media (19% vs. 26% swollen mass at 20 days for 2:1 foam; 32% vs. 50% swollen mass at 20 days for 1:2 foam; and 64% vs. 85% swollen mass at 20 days for 1:1 foam).

4 | DISCUSSION

Using simple polyurethane-based chemistries, we can achieve a SMP hydrogel with high tunability and dual biodegradation mechanisms. Previously PVA has been crosslinked into layered membranes using an isocyanate DSX for islet encapsulation and for self-healing polymers.[33,34] CS-based disulfide materials have also been used to develop nanoparticles for drug delivery.[35] The synthesis method shown in Figure 2 differs from previously published work on disulfide reductive polymers, in that DSXs are typically based on acidic disulfides, such as dithiodipropionic acid.[33,36] Other disulfide crosslinking methods include isocyanate-terminated prepolymers synthesized using materials without pendant OH groups, such as PEG or PCL (i.e., only terminal OH groups), which were then crosslinked using a disulfide-containing polyol.[22,37] In this approach, the disulfide linkages are only located at the ends of prepolymer chains, limiting the overall tunability of the materials. Additionally, using PCL in the crosslinker can have a negative effect on hydrophilicity, swelling, and mechanical properties.[22,37,38] The method we developed here allows for an easy, single-step synthesis of a non-acidic DSX that can be employed with a range of isocyanate-reactive materials, including polyols, such as CS and PVA used here. Using FTIR and gel fraction measurements, we confirmed that this approach successfully crosslinks CS and PVA into a disulfide-containing polyurethane network.

The lower molecular weight PVA 6k hydrogels fabricated using this method generally had higher gel fractions than the PVA 25k gels.

We hypothesize that this result is due to higher mobility of smaller PVA chains, which enables increased interactions with free isocyanates during crosslinking. A similar trend was previously reported in PVA hydrogels crosslinked with glutaraldehyde.[39] Higher gel fractions in the PVA 6k gels correlate with lower porosity values, and the pore size and morphology (Figure 4A) was similar between all the formulations. The density of PVA 6k hydrogels is higher due to increased gel fractions, which reduces overall porosity. In future work, porosity can easily be adjusted by adding more salt particles and/or increasing the size of salts used in the porogen leaching process.

The slight increase in swelling seen with higher CS content can be attributed to the effect that CS has on polymer chain packing. More bulky ring structures and branching increases space between polymer chains. A previous study show that a glutaraldehyde-crosslinked PVA starch composite had a slightly higher swelling once the composite was ≥50% starch.[29] Additionally, more rapid swelling was observed with increasing CS content (Figure 2B,C), which also correlates with previous reports.[40]

The tensile modulus of the bulk hydrogel films is very similar to native tissue (Figure 5); colon tissue has a reported elastic modulus between 300–800 kPa.[41] Additionally, the hydrogels show highly elastic behavior with elongation at break of ~150%. This value is ~2.5–3 times larger than that reported in native tissue.[41,42] This biomaterial system has an overall advantage of high synthetic tunability, allowing us to control the modulus of our materials in future work while better matching native tissue elasticity. For example, by changing the type of isocyanate to one with a more bulky structure, such as methylene diphenyl diisocyanate, or by increasing the crosslink density with a higher DSX content, we could easily tune the modulus of our material.[43]

In general, using porous biomaterials allows for ingrowth of host tissue and increased nutrient transport, with the tradeoff of reduced stiffness with the introduction of pores. A dry compressive modulus that is >2 orders of magnitude higher than the wet modulus in this system enables a water-responsive SMP that changes shape after exposure to body temperature water. This property allows us to program a low-profile, compressed foam shape in the wet state and dry the material for high shape fixity (>97%). Theoretically, this material could be delivered via catheter in the compressed form. The quick recovery (within 3 min) can be employed during implantation, so that the material expands after delivery to fill the fistula site. Current natural bioprosthetics that are used in fistula treatment must be preswollen before implantation, which increases overall procedure time.[11] One limitation to water-based shape memory is the long drying time required for fixing. Further studies on the effects of high heat drying will be carried out to optimize translation of these materials. While the water-responsive SMPs do show consistent thermal transitions (T_g's) there is not enough modulus variability above and below the T_g to allow for traditional, thermally-induced dry shape programing.

Degradation of these materials was tuned with both PVA molecular weight and CS content. Polymers containing PVA 6k showed faster degradation compared to PVA 25k hydrogels in DTT-containing media. While the molecular weight of PVA was increased in these scaffolds, the number of available hydroxyls for crosslinking was held constant. This property is reflected in the relatively consistent mechanical properties between PVA 6k and 25 hydrogels. Thus, we hypothesize that the number of crosslinks/per chain leads to a difference in degradation rate. Lower molecular weight PVA will have fewer crosslinks per chain, which will allow for chains to be more easily released from the network. This finding allows for even more tools to tune the degradation rate independently of mechanical properties in future work through the use of additional PVA molecular weights.

In the PVA 6k hydrogels, degradation rates in amylase and/or DTT were consistently increased with increased CS content. However, in the PVA 25k foam in DTT (with or without amylase), CS content at unequal ratios relative to PVA (1:2 and 2:1) led to faster degradation compared with the 1:1 CS:PVA 25k. This result is attributed to the organization of the polymer structure that allows for easier penetration of DTT through more consistent networks.

Amylase is produced by intestinal epithelial cells, and glutathione is a reducing agent that is abundant in the intestinal mucous.[44,45] Thus, these hydrogels have mechanisms for potential degradation by amylase (CS) and by reducing agents (DTX) after implantation into a fistula site. Amylase alone can partially degrade the foams, but degradation quickly reaches a plateau, which is likely the point at which most of the CS has been broken down, leaving behind a PVA network. This property could enable a tunable drug release mechanism in this system in future work. Here, DTT was used as a representative reducing agent to evaluate the ability to degrade the DTX in the hydrogels. DTT was effective at fully degrading the hydrogels, which was expected, as the crosslinkers were degraded to leave behind soluble PVA and CS. Increasing CS content increased degradation rates in DTT, which may be due to increased water interactions (evidenced by faster swelling profiles and increased equilibrium swelling ratios). Combined treatment with DTT and amylase increased the degradation rate in the CS-containing hydrogels, while the 0:1 PVA control hydrogels had similar degradation profiles in DTT regardless of amylase addition. Again, this result is expected since amylase should not affect the PVA backbone.

While this study provides a foundational understanding of the individual attributes of this material platform, DTT is not naturally found in the human body. Additionally, 10 mM DTT provides a much higher concentration than that of reducing agents that would typically be found at in human tissue, as serum levels of reducing-capable thiols range from 0.35 to 0.55 mM.[46,47] Therefore, the measured degradation profiles in DTT are accelerated to provide a big picture understanding of hydrogel structure effects on degradation properties, and real-time degradation must be assessed using physiologically-relevant concentrations of using glutathione. Future studies will also focus on cellular interactions with the materials and on material degradation in the presence of cells to further evaluate the feasibility of using this hydrogel system as a degradable Crohn's fistula filler. The intestinal mucosa is a unique environment in the body that is difficult to replicate in vitro. Thus, real-time degradation studies will be conducted in in vivo models in future work to provide a full understanding of material degradation profiles.

5 | CONCLUSIONS

This study explored the development of CS/PVA hydrogels as a potential biomaterial strategy for future use in Crohn's fistula treatment. By adjusting two parameters of this system (PVA molecular weight and CS content), we can tune material properties. This water-responsive SMP hydrogel has properties that are comparable to native tissue, and it addresses the limitations of current treatment options by providing a mechanism for easy implantation via shape memory properties and eliminating the need for a removal procedure. While this study focuses on the uses of these hydrogels for prospective use in Crohn's fistula healing, the low cost and highly tunable nature of the material components provides a valuable biomaterial platform with broad potential application in tissue engineering and regenerative medicine applications.

ACKNOWLEDGMENTS

This work was supported by Grants #649526 and 823117 from the Crohn's and Colitis Foundation.

DATA AVAILABILITY STATEMENT

The data that support the findings of this study are available from the corresponding author upon reasonable request.

ORCID

Mary Beth Browning Monroe https://orcid.org/0000-0003-4540-5303

REFERENCES

1. Schwartz DA, Loftus EVJ, Tremaine WJ, et al. The natural history of fistulizing Crohn's disease in Olmsted County, Minnesota. *Gastroenterology*. 2002;122:875-880. doi:10.1053/gast.2002.32362
2. Loftus EVJ. Clinical epidemiology of inflammatory bowel disease: incidence, prevalence, and environmental influences. *Gastroenterology*. 2004;126:1504-1517.
3. Frolkis AD, Dykeman J, Negrón ME, et al. Risk of surgery for inflammatory bowel diseases has decreased over time: a systematic review and meta-analysis of population-based studies. *Gastroenterology*. 2013;145:996-1006. doi:10.1053/j.gastro.2013.07.041
4. Scozzari G, Arezzo A, Morino M. Enterovesical fistulas: diagnosis and management. *Tech Coloproctol*. 2010;14:293-300. doi:10.1007/s10151-010-0602-3
5. West RL, van der Woude CJ, Hansen BE, et al. Clinical and endosonographic effect of ciprofloxacin on the treatment of perianal fistulae in Crohn's disease with infliximab: a double-blind placebo-controlled study. *Aliment Pharmacol Ther*. 2004;20:1329-1336. doi:10.1111/J.1365-2036.2004.02247.X
6. Maralcan G, Başkonuş İ, Gökalp A, Borazan E, Balk A. Long-term results in the treatment of fistula-in-ano with fibrin glue: a prospective study. *J Korean Surg Soc*. 2011;81:169-175. doi:10.4174/JKSS.2011.81.3.169
7. Daodu OO, O'Keefe J, Heine JA. Draining setons as definitive management of fistula-in-ano. *Dis Colon Rectum*. 2018;61:499-503. doi:10.1097/DCR.0000000000001045
8. Present DH. Crohn's fistula: current concepts in management. *Gastroenterology*. 2003;124:1629-1635.
9. Altomare DF, Greco VJ, Tricomi N, et al. Seton or glue for transsphincteric anal fistulae: a prospective randomized crossover clinical trial. *Colorectal Dis*. 2011;13:82-86. doi:10.1111/J.1463-1318.2009.02056.X
10. Loungnarath R, Dietz DW, Mutch MG, Birnbaum EH, Kodner IJ, Fleshman JW. Fibrin glue treatment of complex anal fistulas has low success rate. *Dis Colon Rectum*. 2004;47:432-436. doi:10.1007/S10350-003-0076-8
11. Johnson EK, Gaw JU, Armstrong DN. Efficacy of anal fistula plug vs. fibrin glue in closure of anorectal fistulas. *Dis Colon Rectum*. 2006;49:371-376. doi:10.1007/S10350-005-0288-1
12. Geltzeiler CB, Wieghard N, Tsikitis VL. Recent developments in the surgical management of perianal fistula for Crohn's disease. *Ann Gastroenterol*. 2014;27:320-330. https://pubmed.ncbi.nlm.nih.gov/25331917
13. Narang SK, Jones C, Alam NN, Daniels IR, Smart NJ. Delayed absorbable synthetic plug (GORE® BIO-A®) for the treatment of fistula-in-ano: a systematic review. *Colorectal Dis*. 2016;18:37-44. doi:10.1111/CODI.13208
14. Zhao B, Wang Z, Han J, Zheng Y, Cui J, Yu S. Long-term outcomes of ligation of the inter-sphincteric fistula tract plus bioprosthetic anal fistula plug (LIFT-Plug) in the treatment of trans-sphincteric perianal fistula. *Med Sci Monit*. 2019;25:1350-1354. doi:10.12659/MSM.914925
15. Singhal P, Rodriguez JN, Small W, et al. Ultra low density and highly crosslinked biocompatible shape memory polyurethane foams. *J Polym Sci Part B Polym Phys*. 2012;50:724-737. doi:10.1002/polb.23056
16. Beaman HT, Shepherd E, Satalin J, et al. Hemostatic shape memory polymer foams with improved survival in a lethal traumatic hemorrhage model. *Acta Biomaterialia*. 2022;137:112-123. doi:10.2139/ssrn.3864497
17. Xie M, Wang L, Ge J, Guo B, Ma PX. Strong electroactive biodegradable shape memory polymer networks based on star-shaped polylactide and aniline trimer for bone tissue engineering. *ACS Appl Mater Interfaces*. 2015;7:6772-6781. doi:10.1021/acsami.5b00191
18. Li G, Wang Y, Wang S, Liu Z, Liu Z, Jiang J. A thermo- and moisture-responsive zwitterionic shape memory polymer for novel self-healable wound dressing applications. *Macromol Mater Eng*. 2019;304:1800603. doi:10.1002/mame.201800603
19. Nair LS, Laurencin CT. Biodegradable polymers as biomaterials. *Prog Polym Sci*. 2007;32:762-798. doi:10.1016/j.progpolymsci.2007.05.017
20. Collier JH, Segura T. Evolving the use of peptides as components of biomaterials. *Biomaterials*. 2011;32:4198-4204. doi:10.1016/J.BIOMATERIALS.2011.02.030
21. Meng F, Hennink WE, Zhong Z. Reduction-sensitive polymers and bioconjugates for biomedical applications. *Biomaterials*. 2009;30:2180-2198. doi:10.1016/J.BIOMATERIALS.2009.01.026
22. Jia H, Huang Z, Li Z, Zheng Z, Wang X. One-pot synthesis of highly mechanical and redox-degradable polyurethane hydrogels based-on tetra-PEG and disulfide/thiol chemistry. *RSC Adv*. 2016;6:48863-48869. doi:10.1039/x0xx00000x
23. Nuttelman CR, Henry SM, Anseth KS. Synthesis and characterization of photocrosslinkable, degradable poly(vinyl alcohol)-based tissue engineering scaffolds. *Biomaterials*. 2002;23:3617-3626. doi:10.1016/S0142-9612(02)00093-5
24. Zhang D, Zhou W, Wei B, et al. Carboxyl-modified poly(vinyl alcohol)-crosslinked chitosan hydrogel films for potential wound dressing. *Carbohydr Polym*. 2015;125:189-199. doi:10.1016/j.carbpol.2015.02.034
25. Noè C, Tonda-Turo C, Chiappone A, Sangermano M, Hakkarainen M. Light Processable starch hydrogels. *Polymers*. 2020;12:1359. doi:10.3390/polym12061359
26. Choh S-Y, Cross D, Wang C. Facile synthesis and characterization of disulfide-cross-linked hyaluronic acid hydrogels for protein delivery and cell encapsulation. *Biomacromolecules*. 2011;12:1126-1136. doi:10.1021/bm101451k
27. Aydin AA, Ilberg V. Effect of different polyol-based plasticizers on thermal properties of polyvinyl alcohol:starch blends. *Carbohydr Polym*. 2016;136:441-448. doi:10.1016/J.CARBPOL.2015.08.093
28. Colosi C, Costantini M, Barbetta A, Pecci R, Bedini R, Dentini M. Morphological comparison of PVA scaffolds obtained by gas foaming

and microfluidic foaming techniques. *Langmuir*. 2013;29:82-91. doi:10.1021/la303788z
29. Ramaraj B. Crosslinked poly(vinyl alcohol) and starch composite films. II. Physicomechanical, thermal properties and swelling studies. *J Appl Polym Sci*. 2007;103:909-916. doi:10.1002/app.25237
30. Zhang H, Zhang F, Wu J. Physically crosslinked hydrogels from polysaccharides prepared by freeze–thaw technique. *React Funct Polym*. 2013;73:923-928. doi:10.1016/J.REACTFUNCTPOLYM.2012.12.014
31. Nakano T, Nakaoki T. Coagulation size of freezable water in poly(vinyl alcohol) hydrogels formed by different freeze/thaw cycle periods. *Polym J*. 2011;4311(43):875-880. doi:10.1038/pj.2011.92
32. Wang CL, Lang X, Wu PJ, Casper DP, Li FD. Development of small intestinal enzyme activities and their relationship with some gut regulatory peptides in grazing sheep. *J Anim Sci*. 2017;95:3783-3791. doi:10.2527/jas.2017.1362
33. Teramura Y, Kaneda Y, Iwata H. Islet-encapsulation in ultra-thin layer-by-layer membranes of poly(vinyl alcohol) anchored to poly(ethylene glycol)–lipids in the cell membrane. *Biomaterials*. 2007;28:4818-4825. doi:10.1016/j.biomaterials.2007.07.050
34. Liu M, Zhong J, Li Z, et al. A high stiffness and self-healable polyurethane based on disulfide bonds and hydrogen bonding. *Eur Polym J*. 2020;124:109475. doi:10.1016/J.EURPOLYMJ.2020.109475
35. Zhang A, Zhang Z, Shi F, et al. Disulfide crosslinked PEGylated starch micelles as efficient intracellular drug delivery platforms. *Soft Matter*. 2013;9:2224-2233. doi:10.1039/C2SM27189C
36. Zamboni F, Ryan E, Culebras M, Collins MN. Labile crosslinked hyaluronic acid via urethane formation using bis(β-isocyanatoethyl) disulphide with tuneable physicochemical and immunomodulatory properties. *Carbohydr Polym*. 2020;245:116501. doi:10.1016/J.CARBPOL.2020.116501
37. Lu H, Sun P, Zheng Z, Yao X, Wang X, Chang F-C. Reduction-sensitive rapid degradable poly(urethane-urea)s based on cystine. *Polym Degrad Stab*. 2012;97:661-669. doi:10.1016/j.polymdegradstab.2011.12.023
38. Xu C, Huang Y, Wu J, Tang L, Hong Y. Triggerable degradation of polyurethanes for tissue engineering applications. *ACS Appl Mater Interfaces*. 2015;7:20377-20388. doi:10.1021/acsami.5b06242
39. Alfayyadh AAM, Lotfy S, Basfar AA, Khalil MI. Influences of poly(vinyl alcohol) molecular weight and carbon nanotubes on radiation crosslinking shape memory polymers. *Prog Nat Sci Mater Int*. 2017;27:316-325. doi:10.1016/J.PNSC.2017.04.015
40. Ramaraj B. Crosslinked poly(vinyl alcohol) and starch composite films: study of their physicomechanical, thermal, and swelling properties. *J Appl Polym Sci*. 2007;103:1127-1132. doi:10.1002/APP.24612
41. Davis NF, Mulvihill JJE, Mulay S, Cunnane EM, Bolton DM, Walsh MT. Urinary bladder vs gastrointestinal tissue: a comparative study of their biomechanical properties for urinary tract reconstruction. *Urology*. 2018;113:235-240. doi:10.1016/J.UROLOGY.2017.11.028
42. Christensen MB, Oberg K, Wolchok JC. Tensile properties of the rectal and sigmoid colon: a comparative analysis of human and porcine tissue. *SpringerPlus*. 2015;41(4):1-10. doi:10.1186/S40064-015-0922-X
43. Javni I, Zhang W, Petrović ZS. Effect of different isocyanates on the properties of soy-based polyurethanes. *J Appl Polym Sci*. 2003;88:2912-2916. doi:10.1002/APP.11966
44. Carrière F, Grandval P, Renou C, et al. Quantitative study of digestive enzyme secretion and gastrointestinal lipolysis in chronic pancreatitis. *Clin Gastroenterol Hepatol*. 2005;3(1):28-38. doi:10.1053/S1542-3565
45. Loguercio C, Di Pierro M. The role of glutathione in the gastrointestinal tract: a review. *Ital J Gastroenterol Hepatol*. 1999;31:401-407.
46. Giustarini D, Dalle-Donne I, Lorenzini S, Milzani A, Rossi R. Age-related influence on thiol, disulfide, and protein-mixed disulfide levels in human plasma. *J Gerontol Ser A Biol Sci Med Sci*. 2006;61:1030-1038. doi:10.1093/gerona/61.10.1030
47. Dirican N, Dirican A, Sen O, et al. Thiol/disulfide homeostasis: a prognostic biomarker for patients with advanced non-small cell lung cancer? *Redox Rep*. 2016;21:197-203. doi:10.1179/1351000215Y.0000000027

How to cite this article: Beaman HT, Howes B, Ganesh P, Monroe MBB. Shape memory polymer hydrogels with cell-responsive degradation mechanisms for Crohn's fistula closure. *J Biomed Mater Res*. 2022;1-12. doi:10.1002/jbm.a.37376